CORE
Metadata, citation and similar papers at core.ac.uk

AIP | Applied Physics Letters

Control of the electrode work function and active layer morphology via surface modification of indium tin oxide for high efficiency organic photovoltaics

Jong Soo Kim, Jong Hwan Park, Ji Hwang Lee, Jang Jo, Dong-Yu Kim, and Kilwon Cho

Citation: Applied Physics Letters **91**, 112111 (2007); doi: 10.1063/1.2778548
View online: http://dx.doi.org/10.1063/1.2778548
View Table of Contents: http://scitation.aip.org/content/aip/journal/apl/91/11?ver=pdfcov
Published by the AIP Publishing

Articles you may be interested in

High work function transparent middle electrode for organic tandem solar cells
Appl. Phys. Lett. **96**, 153504 (2010); 10.1063/1.3387863

Tailoring the work function of indium tin oxide electrodes in electrophosphorescent organic light-emitting diodes
J. Appl. Phys. **105**, 084507 (2009); 10.1063/1.3095492

Effect of phosphonic acid surface modifiers on the work function of indium tin oxide and on the charge injection barrier into organic single-layer diodes
J. Appl. Phys. **105**, 074511 (2009); 10.1063/1.3095490

Induced increase in surface work function and surface energy of indium tin oxide-doped ZnO films by (N H 4) 2 S x treatment
J. Appl. Phys. **101**, 113713 (2007); 10.1063/1.2745366

Characterization of organic photovoltaic devices with indium-tin-oxide anode treated by plasma in various gases
J. Appl. Phys. **100**, 093711 (2006); 10.1063/1.2372574

This article is copyrighted as indicated in the article. Reuse of AIP content is subject to the terms at: http://scitation.aip.org/termsconditions. Downloaded to IP: 141.223.173.110 On: Tue, 21 Apr 2015 11:18:30

Control of the electrode work function and active layer morphology via surface modification of indium tin oxide for high efficiency organic photovoltaics

Jong Soo Kim, Jong Hwan Park, and Ji Hwang Lee
Department of Chemical Engineering, School of Environmental Science and Engineering, Pohang University of Science and Technology, Pohang 790-784, Korea

Jang Jo and Dong-Yu Kim
Department of Materials Science and Engineering, Gwangju Institute of Science and Technology (GIST), Gwangju 500-712, Korea

Kilwon Cho[a)]
Department of Chemical Engineering, School of Environmental Science and Engineering, Pohang University of Science and Technology, Pohang 790-784, Korea

(Received 30 July 2007; accepted 10 August 2007; published online 13 September 2007)

Indium tin oxide (ITO) substrates modified with self-assembled monolayers (SAMs) were used to control the anode work function and active layer morphology of organic solar cells based on poly(3-hexylthiophene)/[6:6]-phenyl-C61 butyric acid methyl ester heterojunctions. By using SAMs with the terminal groups $-NH_2$, $-CH_3$, and $-CF_3$, the authors were able to control the hole injection barrier of the ITO closer to the highest occupied molecular orbital level of active layer and surface energy of the ITO substrate. A solar cell device with CF_3 SAM treated ITO was found to exhibit high efficiency performance, about 3.15%. © *2007 American Institute of Physics*.
[DOI: 10.1063/1.2778548]

Bulk heterojunction organic photovoltaics (OPVs) based on organic materials have recently been intensively investigated with a view to increasing their efficiency.[1–4] Like other organic electronic devices,[5–7] charge injection at the organic-inorganic interface is a key issue for OPVs.[8,9] Surface treatments of electrode including oxidation, the addition of a self-assembled layer,[10–14] or poly(3,4-ethylene dioxythiophene): poly(styrene-sulfonate) (PEDOT:PSS) layer insertion[15] can lower or raise the work functions of cathodes and anodes, or enhance the cohesion, and thus lower the interfacial series resistance. However, the effects on OPV device performance of shifting the electrode's work function and altering the active layer's structure that result from changing the surface energy of the indium tin otide (ITO) electrode have not previously been reported. In bulk heterojunction solar cells using poly(3-hexylthiophene) doped [6:6]-phenyl-C61 butyric acid methyl ester (P3HT:PCBM), morphology control of active layer is very important. Additionally, through thermal annealing of P3HT:PCBM blend devices, the external quantum efficiency and power conversion efficiency of these cells are dramatically increased;[16] In these cases, a power conversion efficiency for a P3HT/PCBM blend system as high as about 3% has been reported.[17] Many studies have shown that poor morphology, i.e., the severe phase separation of the active layer, is a key factor in loss of device performance.[18]

In this study, we modified the surface characteristics of ITO substrates by carrying out self-assembled monolayer (SAM) treatments, and investigated the effects of these treatments and thermal annealing on the morphology of the active layer, the work function of the ITO electrode, and the resulting OPV device performance. These results are useful for optimizing device structure and improving OPV performance.

Hydroxyl groups were introduced onto the ITO substrate by carrying out Ar plasma treatment, and other functional groups were introduced through various SAM treatments with silane compounds, i.e., *N*-propyltriethoxysilane for the CH_3 SAM, trichloro(3,3,3-trifluoropropylsilane) for the CF_3 SAM, and aminopropyl triethoxysilane for the NH_2 SAM. With these modifications, we were able to control the charge injection barrier and the wettability of the ITO glass. The surface energies of the various SAM-treated ITO substrates were determined from contact angle measurements using distilled water and diiodomethane as probe liquids, and the geometric mean equation, $(1+\cos\theta)\gamma_{pl}=2(\gamma_s^d\gamma_{pl}^d)^{1/2}+2(\gamma_s^p\gamma_{pl}^p)^{1/2}$,

TABLE I. Surface energies of the various SAM-treated ITO substrates and the electrical properties of the corresponding OPV devices.

	Relative work function	Surface energy (mJ/m^2)	V_{oc} (V)	J_{sc} (mA/Cm^2)	FF	η (%)
Untreated	4.7	69.2				
As prepared			0.39	5.38	0.35	0.73
Annealed			0.36	5.98	0.35	0.75
NH_2 SAM	4.35	46.5				
As prepared			0.38	3.63	0.38	0.53
Annealed			0.55	5.71	0.30	0.95
CH_3 SAM	3.87	31.4				
As prepared			0.41	1.46	0.35	0.21
Annealed			0.57	6.82	0.32	1.24
CF_3 SAM	5.16	28.7				
As prepared			0.57	6.20	0.37	1.29
Annealed			0.60	13.87	0.38	3.15

[a)]Author to whom correspondence should be addressed; electronic mail: kwcho@postech.ac.kr

This article is copyrighted as indicated in the article. Reuse of AIP content is subject to the terms at: http://scitation.aip.org/termsconditions. Downloaded to IP: 141.223.173.110 On: Tue, 21 Apr 2015 11:18:30

 © 2007 American Institute of Physics

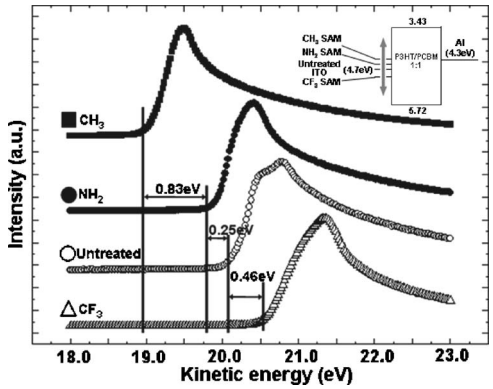

FIG. 1. Secondary electron emission spectra for the various ITO substrates: CH_3 SAM treated (closed rectangles), NH_2 SAM treated (closed circles), untreated (open circles), and CF_3 SAM treated (open triangles). Inset: schematic energy level diagram of the electron-donating and electron-withdrawing SAM treated ITOs.

where γ_s and γ_{pl} are the surface energies of the sample and the probe liquid respectively, and the superscripts d and p refer to the dispersion and polar (nondispersion) components of the surface energy, respectively. The surface energies of the various SAM-treated ITO substrates are summarized in Table I.

The modification of the ITO substrate has two major effects on P3HT:PCBM heterojunction solar cell devices, i.e., changes in the hole injection barrier because of changes in the work function of ITO, and changes in the morphology of the active layer. First, we characterized the work functions of the modified ITO substrates. The work function of bare ITO is known to be 4.7 eV. As a result of the addition of the SAMs onto the ITO glass substrates, work function shifts were observed. The alteration in the work function of each substrate was measured using secondary electron emission spectroscopy (Fig. 1) at the 4B1 beam lines at the Pohang Accelerator Laboratory, Korea. The secondary electron spectrum can be used to determine the change in the work function of an electrode and its relative charge distribution. The onset of photoemission corresponds to the change in the work function at the ITO surface and was measured with a negative bias (−20 V) on the sample. The onset of secondary electrons was determined by extrapolating two solid lines from the background and straight onset in each spectrum. As can be seen in Fig. 1, the onset of secondary electrons in the CH_3 SAM treated ITO substrate occurs at a kinetic energy that is 1.08 eV lower than the onset for the same substrate without any treatment. In the case of the CF_3 terminated SAM, the onset of secondary electrons is 0.46 eV higher than that of the untreated surface. Thus there is a 1.54 eV gap between the CH_3 and CF_3 SAM treated ITO substrates. This result indicates that the work function of the CH_3 SAM treated ITO substrate is lower than that of the CF_3 SAM treated ITO substrate by 1.54 eV. By using this treatment with its resulting work function shifts, we can control the ITO work function such that it is near the active layer's highest occupied molecular orbital (HOMO) level, and then hole injection from the active layer to the anode is facilitated and we can expect the device with CF_3 SAM treated ITO glass to have a higher efficiency.

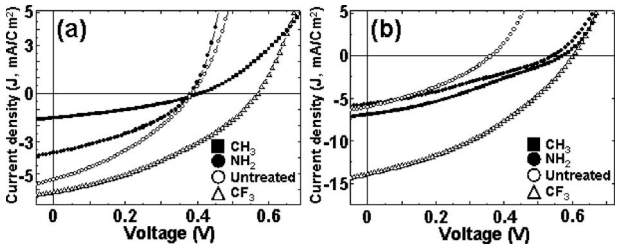

FIG. 2. *J-V* characteristics (AM1.5, 100 mW/Cm^2) of the OPV devices with the various SAM-treated ITO substrates: (a) as prepared and (b) annealed at 150 °C for 20 min.

In order to analyze the electrical properties of the various SAM-treated ITO surfaces, an active layer composed of 1 wt % P3HT/PCBM blend (1:1) in chlorobenzene was spin coated onto the modified ITO substrates. To measure the performances of solar cells using these ITO substrates, current density–voltage (*J-V*) characteristics were measured in the dark and under AM1.5 solar illumination (with reference to reference cell PVM 132 calibrated with NREL) at an intensity of 100 mW/cm^2 with an Oriel 1 kW solar simulator using a programable Keithley mode 4200 power source. All electrical measurements and active layer fabrication were executed under the inert nitrogen gas. The samples' efficiencies were relatively low, i.e., less than 1.3% in most cases without annealing [Fig. 2(a)]. The device efficiency increases in the following order: $CH_3 < NH_2 <$ untreated $< CF_3$. Since the morphology and crystalline structure of the active layer are not significantly different for these ITO glasses before thermal annealing (Figs. 3 and 4), we conclude that the easier hole injection into the anode (ITO) increases the efficiency of the CF_3 SAM treated ITO glasses.

However, after annealing, the devices with the variously treated substrates exhibit very different device efficiencies. Further, the morphologies of the active layers on the various ITO substrates are quite different after thermal annealing. The efficiency of the device with untreated ITO glass does not change after thermal annealing. However, for the devices with the other SAM-treated ITO glasses, the efficiencies increase after annealing (Table I). As shown in Fig. 5, the optical microscopy images of the samples are quite different, depending on which SAM is present, after annealing (150 °C, 20 min). Little phase separation of the P3HT/PCBM blends occurs for the hydrophobic CH_3 and CF_3

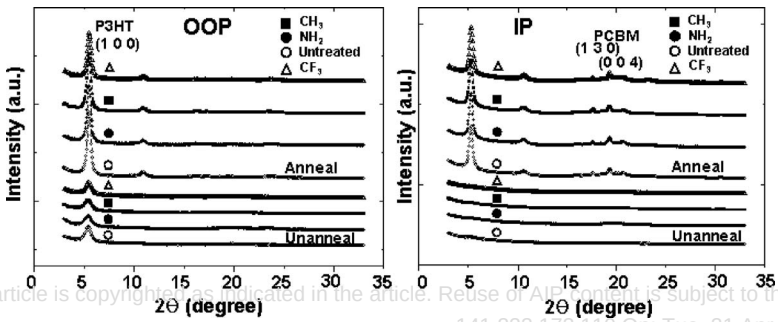

FIG. 3. (a) Out-of-plane XRD patterns for the P3HT/PCBM active layer for the various surface-treated ITOs. (b) In-plane XRD patterns for the P3HT/PCBM active layer for the various surface-treated ITOs.

This article is copyrighted as indicated in the article. Reuse of AIP content is subject to the terms at: http://scitation.aip.org/termsconditions. Downloaded to IP: 141.223.173.110 On: Tue, 21 Apr 2015 11:18:30

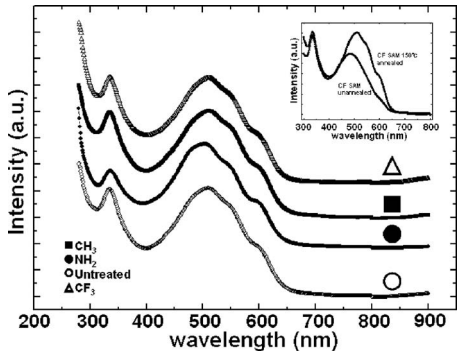

FIG. 4. UV absorption spectra of the P3HT/PCBM active layer for the various surface-treated ITOs; the intensity and peak shift do not vary for the various surface treatments. Inset: comparison of UV absorption spectra of the P3HT/PCBM active layer for the CF_3 SAM treated ITOs between unannealed and annealed samples.

SAM treated surfaces. However, in the case of the hydrophilic OH-terminated ITO substrate and the relatively hydrophilic surface of the NH_2 SAM treated surface, very severe phase separation occurs, and aggregated PCBM forms a dispersed phase. However, the in-plane and out-of-plane x-ray diffraction (XRD) results for the active layer do not indicate that there is any variation in the molecular ordering of P3HT in spite of the variation in surface character, even though the phase separation in the macrophase is quite different in each case.

Through annealing process, OPV devices benefit in two ways from the better electron transport of the PCBM clusters and the enhanced absorption properties of the P3HT crystallites. However, when the active layer is coated onto the hydrophilic group treated surface, the extreme phase separation results in a lower power conversion efficiency in spite of the improvement in the hole injection barrier. In contrast, the hydrophobic terminal groups result in higher power conversion efficiency, i.e., ~1.29% for the CH_3 SAM treated surface and ~3.15% for the CF_3 SAM treated surface [Fig. 2(b)]. Even if a device has improved hole injection to the anode, poor bulk heterojunction structure between the donor and acceptor materials caused by higher surface energy of the ITO substrate, and excessive phase separation mean that better device performance is not possible. Therefore, the CF_3 SAM treated sample has improved hole injection into the ITO and the optimum active layer phase separation, and was found to have the highest efficiency in these experiments. This result is comparable to that for a device

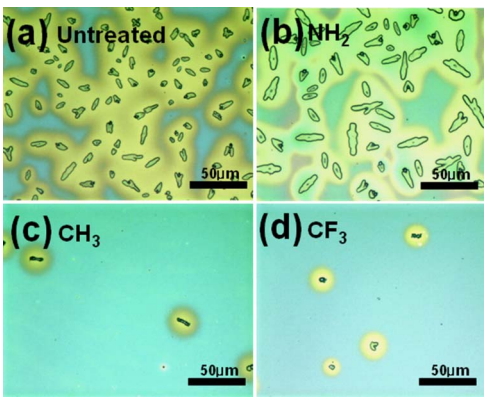

FIG. 5. (Color online) Optical microscopy images of P3HT:PCBM (1:1) blends on various ITO glasses after annealing at 150 °C for 20 min. The thickness of the blend film is about 120 nm. (a) Untreated, (b) NH_2, (c) CH_3, and (d) CF_3 SAM treated ITO substrates.

with a PEDOT/PSS insertion layer. Considering the hole injection barrier and the surface energy, the device with a CF_3 SAM treated ITO substrate should have a higher efficiency than a device with a PEDOT/PSS insertion layer. The reason why the CF_3 SAM treated sample does not have better device performance is that the CF_3 SAM treated sample could not compensate for the roughness of ITO (~2 nm) than PEDOT/PSS layer.

In summary, we have correlated the changes in electrode work function and active layer structure due to the surface energy change produced by treating ITO with various SAMs with the electrical properties of OPVs. SAMs with electron-withdrawing groups increase the work function of the ITO/active layer interface more than SAMs with electron-donating groups. However, the phase separation of the active layer is a more important factor than the match between the injection barrier and the active layer's HOMO level. The best power conversion efficiency value we obtained was 3.15% for a CF_3 SAM treated surface after annealing, in the absence of a PEDOT:PSS layer. By carrying out further optimization of this device, we expect to increase the performance of devices obtained by SAM treatment of ITO substrates.

This work was supported by the ERC Program (R11-2003-006-03005-0) of the MOST, a grant (F0004022-2006-22) from the Information Display R&D Center under the 21st Century Frontier R&D Program, the BK21 Program of the Ministry of Education and Human Resources Development of Korea, and the Pohang Accelerator Laboratory by providing the 4B1 and 10C1 beam lines used in this study.

[1] L. H. Nguyen, H. Hoppe, T. Erb, S. Gunes, G. Gobsch, and N. S. Sariciftci, Adv. Funct. Mater. **17**, 1071 (2007).
[2] Y. Kim, S. A. Choulis, J. Nelson, D. D. C. Bradley, S. Cook, and J. R. Durrant, J. Mater. Sci. **40**, 1371 (2004).
[3] J. Huang, G. Li, and Y. Yang, Appl. Phys. Lett. **87**, 112105 (2005).
[4] U. Zhokhavets, T. Erb, H. Hoppe, G. Gobsch, and N. S. Sariciftci, Thin Solid Films **496**, 679 (2006).
[5] J. H. Cho, H. S. Lee, Y. S. Jang, Y. K. Lee, S. K. Kwon, J. Jang, and K. Cho, Appl. Phys. Lett. **89**, 083508 (2006).
[6] N. Koch, A. Elschner, J. P. Rabe, and R. L. Johnson, Adv. Mater. (Weinheim, Ger.) **3**, 330 (2005).
[7] H. Ishii, K. Sugiyama, E. Ito, and K. Seki, Adv. Mater. (Weinheim, Ger.) **11**, 605 (1999).
[8] Y. S. Jang, J. H. Cho, D. H. Kim, Y. D. Park, M. K. Hwang, and K. Cho, Appl. Phys. Lett. **90**, 132104 (2007).
[9] I. H. Campbell, S. Rubin, T. A. Zawodzinski, J. D. Kress, R. L. Martin, D. L. Smith, N. N. Barashkov, and J. P. Ferraris, Phys. Rev. B **54**, 14321 (1996).
[10] S. Kobayashi, T. Nishikawa, T. Takenobu, S. Mori, T. Shimoda, T. Mitani, H. Shimitani, N. Yoshimoto, S. Ogawa, and Y. Iwasa, Nat. Mater. **3**, 317 (2004).
[11] S. Khodabakhsh, D. Poplavskyy, S. Heutz, J. Nelson, D. D. C. Bradley, H. Murata, and T. S. Jones, Adv. Funct. Mater. **14**, 1205 (2004).
[12] B. de Boer, A. Hadipour, M. M. Mandoc, T. van Woudenbergh, and P. W. M. Blom, Adv. Mater. (Weinheim, Ger.) **17**, 621 (2005).
[13] E. L. Hanson, J. Guo, N. Koch, J. Schwartz, and S. L. Bernasek, J. Am. Chem. Soc. **127**, 10058 (2005).
[14] S. E. Koh, K. D. McDonald, D. H. Holt, and C. S. Dulcey, Langmuir **22**, 6249 (2006).
[15] S. E. Saheen, C. J. Brabec, N. S. Sariciftci, F. Padinger, T. Fromberz, and J. C. Hummelen, Appl. Phys. Lett. **78**, 841 (2001).
[16] D. Chirvase, Z. Chiguvare, M. Knipper, J. Parisi, V. Dyakonov, and J. C. Hummelen, J. Appl. Phys. **93**, 3376 (2003).
[17] Y. Kim, S. A. Choulis, J. Nelson, D. D. C. Bradley, S. Cook, and J. R. Durrant, Appl. Phys. Lett. **86**, 063502 (2005).
[18] A. Swinnen, I. Haeldermans, M. vande Ven, J. D'haen, G. Vanhoyland, S. Aresu, M. D'Olieslaeger, and J. Manca, Adv. Funct. Mater. **26**, 760 (2006).

This article is copyrighted as indicated in the article. Reuse of AIP content is subject to the terms at: http://scitation.aip.org/termsconditions. Downloaded to IP: 141.223.173.110 On: Tue, 21 Apr 2015 11:18:30